FaST - Jurnal Sains dan Teknologi, Vol. 10, No.1, Mei 2026
e-ISSN 2598-9596
DOI: https://doi.org/10.19166/fastjst.v10i1.10486
Available online at: https://ojs.uph.edu/index.php/FaSTJST/article/view/10486

3D-Printed Porous Tantalum Scaffolds for Bone Regeneration: A Narrative Review of Structural Design, Biological Performance, and Clinical Applications

Michael Lizar[1*)], Xingshuang Ma[1)]
[1]The Key Laboratory of Biorheological Science and Technology, Ministry of Education, College of Bioengineering, Chongqing University, Chongqing 400044, China

ABSTRACT

Bone fractures remain a major clinical challenge in orthopedic surgery, requiring biomaterials that closely mimic the structural and mechanical properties of native bone. Although titanium and its alloys are widely used, their limited porosity and elastic modulus mismatch may compromise osseointegration and long-term implant stability. Three-dimensional (3D)-printed porous tantalum (Ta) scaffolds have emerged as promising alternatives due to their high biocompatibility, corrosion resistance, and osteoconductive potential. This narrative review comprehensively evaluates the structural design, additive manufacturing strategies, mechanical performance, biological interactions, and clinical applications of 3D-printed porous Ta scaffolds for bone regeneration. Particular attention is given to scaffold architecture, pore geometry optimization, and scaffold–cell interactions, including the incorporation of bone marrow–derived mesenchymal stem cells (BMSCs). Advances in additive manufacturing techniques, such as Selective Laser Melting and Laser Engineered Net Shaping, enable the fabrication of highly interconnected porous structures with bone-mimetic mechanical properties. Evidence from in vitro and in vivo studies indicates that pore sizes of 400–600 μm and porosity around 80% provide a favorable microenvironment for cell adhesion, proliferation, and osteogenic differentiation. Functionalization strategies and activation of osteogenic signaling pathways further enhance mineralization and interfacial integration. Overall, the integration of 3D-printed porous Ta scaffolds with regenerative cellular strategies represents a promising approach for bone defect repair, spinal fusion, and joint reconstruction. Continued optimization of scaffold design and validation through long-term clinical studies are essential to facilitate translational application.

ARTICLE INFO

Keywords: additive manufacturing; bone regeneration; mesenchymal stem cells; porous tantalum; tissue engineering

***Corresponding author**:
michaelizar@gmail.com

Article history:
Submitted 07 Jan 2026
Revised 18 Feb 2026
Accepted 23 Feb 2026
Online Available 17 Apr 2026
Published 20 May 2026

1. Introduction

Bone fractures in orthopedics represent a complex clinical challenge, particularly in significant segmental defects, delayed union, or compromised bone quality. Effectively managing these conditions requires bone implants that provide mechanical support, biological integration, and enhanced bone regeneration. Traditionally, metallic biomaterials such as titanium (Ti) and its alloys have been widely used due to their mechanical strength and corrosion resistance. However, Ti exhibits several limitations, including low volumetric porosity, a relatively high elastic modulus, and limited osseointegration, leading to stress shielding and implant failure. Tantalum (Ta) has emerged as a promising alternative biomaterial in recent years due to its excellent biocompatibility, high volumetric porosity, and mechanical properties that closely mimic cancellous bone. These characteristics support its use in various orthopedic applications. Clinical success has been demonstrated particularly in procedures such as tibial tubercle advancement, where porous tantalum has shown outcomes comparable to autologous bone grafts, with reduced complications and improved patient satisfaction [1]. Broader applications, including hip and knee arthroplasty, osteonecrosis treatment, and spinal fusion, have also shown promising results, as reported in other studies [2]. The development of additive manufacturing (AM) technologies, or 3D printing, has further enabled the precise fabrication of porous Ta scaffolds with controlled geometry and tailored mechanical properties [3]. Bone remodelling is regulated by a dynamic balance between bone formation and resorption, involving osteoblasts, osteocytes, and osteoclasts. Osteoblasts synthesize the bone matrix, osteocytes in the matrix serve as mechanosensors, and osteoclasts resorb bone to maintain skeletal homeostasis [4,5,6]. Disruption in this balance leads to impaired healing, particularly in challenging fracture environments (**Fig. 1**). Advances in regenerative medicine have introduced mesenchymal stem cells (MSCs), particularly those derived from bone

FaST - Jurnal Sains dan Teknologi, Vol. 10, No.1, Mei 2026
e-ISSN 2598-9596
DOI: https://doi.org/10.19166/fastjst.v10i1.10486
Available online at: https://ojs.uph.edu/index.php/FaSTJST/article/view/10486

marrow (BMSCs), as a powerful tool for enhancing osteogenesis. When combined with porous Ta scaffolds, MSCs contribute to both structural support and biological functionality. This review evaluates the potential of 3D-printed porous Ta scaffolds integrated with MSCs, focusing on fabrication methods, biological performance, and clinical relevance in bone regeneration.

2. Review Methodology

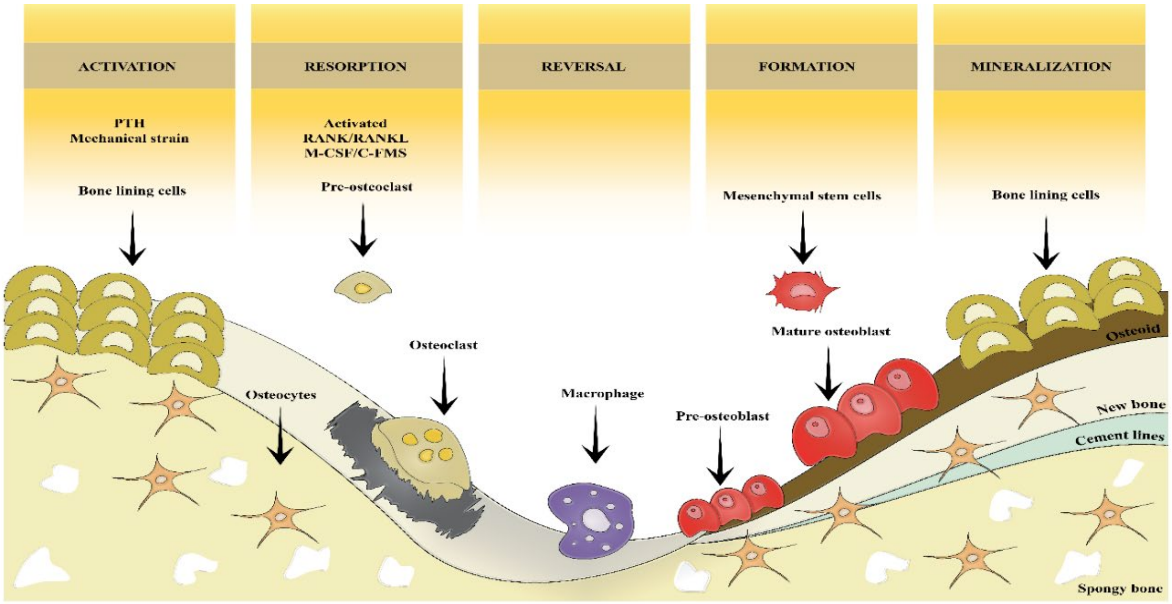

Figure 1. Bone remodeling process consists of five phases: activation, resorption, reversal, formation, and mineralization.

The research was carried out as a narrative review. The terms "porous tantalum," "3D printing," "additive manufacturing," "bone regeneration," "osseointegration," and "mesenchymal stem cells" were combined to search PubMed, Scopus, and Web of Science databases for pertinent peer-reviewed publications published between January 2010 and December 2025. Translational research, clinical studies including orthopedic and dental applications, in vitro studies, and in vivo animal models were prioritized. Articles that just discussed titanium and made no analogy to tantalum were not included. Methodological rigor, relevance to scaffold construction, mechanical performance, biological results, and clinical translation were all prioritized throughout the selection process. After screening titles and abstracts for relevance, studies were selected based on thematic relevance and methodological quality. Duplicate records were excluded

2.1 3D Printing Techniques for Bone Implants

Earlier scaffold fabrication methods, including metal-fiber and powder metallurgy-based loose sintering and plasma spraying, often result in inconsistent pore geometry, non-uniform porosity, and poor interconnectivity. For example, Torres et al. (2014) highlighted irregular pore structures using conventional PM, and Wauthle et al. (2015) pointed out that these older techniques cannot produce the fully connected porous architectures achievable with additive manufacturing [7,8]. These shortcomings often compromise scaffold functionality, mechanical strength, and biological performance. Additionally, conventional approaches lack the precision and adaptability to fabricate patient-specific implants with complex geometries. To address these challenges, additive manufacturing (AM), also known as 3D printing, has emerged as a transformative technology in orthopedic biomaterials. AM enables the direct fabrication of complex, customized structures based on computer-aided design (CAD) models. Its advantages include tunable pore size, high structural accuracy, shortened production time, and potential scalability for clinical use [9,10,11]. These features make AM highly suitable for producing implants replicating natural bone's mechanical and architectural properties. Metal-based AM technologies for scaffold fabrication fall into two primary categories: powder bed fusion (PBF) and directed energy deposition (DED) (**Fig. 2**).

FaST - Jurnal Sains dan Teknologi, Vol. 10, No.1, Mei 2026
e-ISSN 2598-9596
DOI: https://doi.org/10.19166/fastjst.v10i1.10486
Available online at: https://ojs.uph.edu/index.php/FaSTJST/article/view/10486

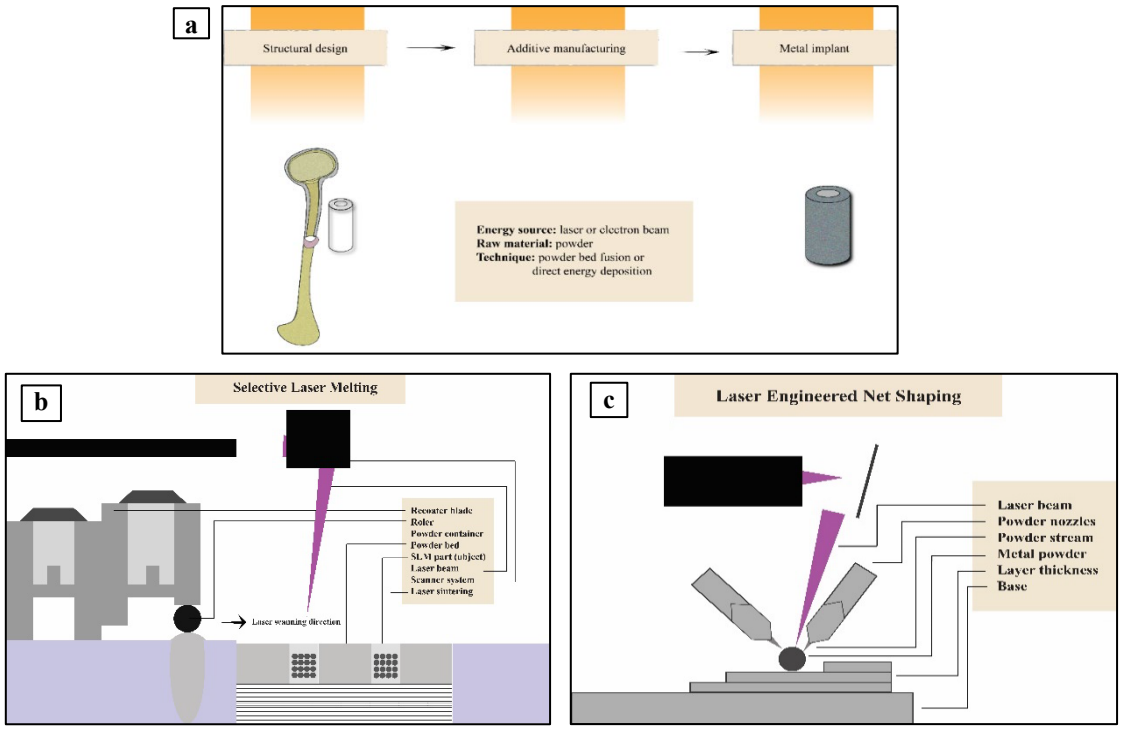

Figure 2 Additive manufacturing process. (a) The steps of the manufacturing process of metal materials; (b) Selective Laser Melting (SLM); (c) Laser Engineered Net Shaping (LENS)

In PBF systems, such as selective laser sintering (SLS), selective laser melting (SLM), electron beam melting (EBM), and direct metal laser sintering (DMLS), a high-energy beam selectively fuses layers of metal powder to build the scaffold layer by layer. These techniques offer high resolution and excellent control over porosity and interconnectivity. In contrast, DED methods, including laser engineered net shaping (LENS), direct metal deposition (DMD), and 3D fiber deposition, simultaneously deposit and melt metal powders onto a substrate [12,13]. LENS, for instance, uses a laser to create a melt pool into which metal powder is injected, enabling precise control over deposition and layer bonding. SLM is particularly effective in creating fully dense metal structures with well-defined pore networks, while LENS excels at producing functionally graded or hybrid structures with tailored mechanical properties. SLM [14,15] and LENS [16,17] have been successfully applied to fabricate porous tantalum scaffolds, offering reproducibility and versatility for orthopedic applications (**Table 1**) [18,19]. Their ability to produce scaffolds with optimal pore sizes (typically 300–600 µm) and high porosity (70–90%) allows for improved cell infiltration, vascularization, and load-bearing capacity. These technologies lay the groundwork for next-generation scaffolds that integrate mechanical strength with biological function, especially when combined with mesenchymal stem cells (MSCs) for enhanced osteogenesis.

Table 1 Additive Manufacturing Techniques

Methods	Process Characteristics	Type Materials	Category	Advantages	Limitations
SLM [14,15]	Preparing the powder bed Layer-by-layer addition of the powder A laser beam is used to melt the thin layer of metal powder	Metal powder	Powder bed fusion	High density, High processing with controlled pore interconnectivity and porosity	Costly Relatively slow process
LENS [16,17]	Metal substrate deposition The high-power laser beams are used to melt metal powder	Metal powder	Directed energy deposition	Ability to tailor the deposition parameter with a high degree of control	Higher residual stress

FaST - Jurnal Sains dan Teknologi, Vol. 10, No.1, Mei 2026
e-ISSN 2598-9596
DOI: https://doi.org/10.19166/fastjst.v10i1.10486
Available online at: https://ojs.uph.edu/index.php/FaSTJST/article/view/10486

Inert shroud gas is used to shield the melt pool	Fully dense shapes and excellent material properties

Several critical factors must be considered in developing 3D-printed porous metal scaffolds, including material selection, pore size, porosity, pore structure, surface modification, and mechanical strength. These parameters can be precisely designed and evaluated using AM technologies before mass production. As a bio-inert metal, tantalum exhibits excellent biocompatibility, favorable mechanical properties, and safety for biomedical applications [20]. AM-produced porous Ta scaffolds offer controlled pore architecture, a key determinant in bone ingrowth. The CAD-based design enables predefinition of interparticle pore geometry, directly influencing the scaffold's mechanical behavior and osteoconductive properties [21]. Optimal scaffold designs should incorporate interconnected pores that facilitate vascularization and nutrient transport while maintaining mechanical integrity. Studies suggest effective pore sizes for bone in-growth range from 100 µm to over 400 µm [20,21]. Cheng et al. found that larger pores (653 µm) enhance osteogenic differentiation [22], while Biemond et al. observed improved bone formation in scaffolds with pore sizes of 1200 µm compared to 900 µm [23]. Pore throat size, the narrowest passage linking adjacent pores, critically influences cellular infiltration and nutrient transport. Narrow throats impede oxygen and cell penetration, while huge ones can hinder uniform bone coverage and integration [24,25]. Porosity, defined as the volume percentage of void space in the scaffold, is closely linked to pore size, strut thickness, and lattice geometry. Human trabecular bone typically exhibits porosity between 70% and 90%. Scaffolds mimicking this porosity range (e.g., 80% in porous Ta) balance bone ingrowth potential and mechanical performance, maintaining elastic moduli in the 2.5–4 GPa [26,27]. The pore structure is also vital in determining compressive strength and biological performance. AM enables consistent pore geometry, such as wave, diamond, or cubic structures, through CAD modeling, overcoming the limitations of traditional fabrication methods [28, 29]. Biemond et al. reported that wave structures enhance mechanical interlocking via increased friction, whereas cubic geometries improve in vivo bone ingrowth [23]. Diamond lattice structures favor cell attachment and proliferation due to their interconnected architecture and uniform stress distribution [30]. In addition to geometry, surface modification techniques are critical in enhancing scaffold bioactivity and long-term integration. Methods such as anodization, calcium phosphate coatings, and hydrothermal treatments can improve osteoinductivity and reduce the risk of implant rejection by promoting stronger interactions with host tissue [31,32]. Mechanical properties, including load-bearing capacity, fatigue resistance, and mitigation of stress shielding, are also vital for ensuring the long-term functionality of orthopedic implants. Additively manufactured (AM) scaffolds designed with open, non-stochastic lattice architectures, such as diamond or gyroid topologies, have demonstrated superior mechanical stability and enhanced biological integration, making them promising candidates for load-bearing bone applications [33].

2.2 Biocompatibility & Comparative Scaffold Studies

The structural architecture and mechanical performance of porous tantalum scaffolds play a central role in their biological functionality and clinical reliability. Parameters such as pore size, porosity, interconnectivity, surface modification, and fabrication technique directly influence compressive strength, elastic modulus, and osteoconductive behavior. A synthesis of reported design configurations and mechanical benchmarks for 3D-printed porous tantalum scaffolds is summarized in (**Table 2**).

Table 2 Comparative Study of Recent Studies of 3D-Printed Porous Tantalum

Study	Fabrication	MSC Integration	Scaffold Modification	Model	Results
Zhang et al. (2023) [96]	SLM-printed PTa with hydrothermal nano-topography	Rat BMSCs (in vitro)	Nano-structured surface via alkali–heat–hydrothermal treatment	Rabbit mandibular defect (in vivo)	Nano-topography significantly enhanced BMSC adhesion, osteogenic differentiation (↑ALP, mineralization), and early bone formation.

FaST - Jurnal Sains dan Teknologi, Vol. 10, No.1, Mei 2026
e-ISSN 2598-9596
DOI: https://doi.org/10.19166/fastjst.v10i1.10486
Available online at: https://ojs.uph.edu/index.php/FaSTJST/article/view/10486

Liu et al. (2025) [97]	3D-printed PTa with polydopamine; MZIF-8 drug delivery	BMSC regulation via macrophage polarization	Polydopamine + MZIF-8 + melatonin for immunoregulatory release	Osteoporotic rat femur (in vivo)	Promoted M2 macrophage shift, inhibited inflammation, enhanced BMSC osteogenesis via P38-MAPK
Jiao et al. (2023) [98]	SLM-printed PTa scaffolds (60%, 70%, 80% porosity)	Rat BMSCs (in vitro)	Varying porosity only	Rat femoral defect (in vivo)	70–80% porosity provided maximal BMSC proliferation, osteogenic gene expression, and bone ingrowth; 70% porosity was optimal
Yu et al. (2024) [99]	SLM-printed PTa with corrosion-resistant surface	Human BMSCs (in vitro)	Review of customized PTa (no specific coating)	-	Confirmed high BMSC proliferation, osteogenesis, corrosion resistance, and overall biocompatibility
Zhao et al. (2025) [100]	Porous Ta integrated with gelatin nanoparticle (GNP) hydrogel	BMSC + endothelial co-culture	GNP hydrogel for growth factor delivery and angiogenesis	In vivo vascularized bone model	Promoted both osteogenesis and angiogenesis, indicating vascularized bone regeneration

The selection of biologically compatible and mechanically reliable materials is essential to support bone remodeling. An ideal implant material should mimic the elastic modulus of bone, offer sufficient mechanical strength, induce osteogenesis, and remain inert within the physiological environment [34]. Tantalum (Ta), a rare transition metal with atomic number 73, has been utilized in biomedical applications since the 1940s due to its unique properties, including high corrosion resistance, a relatively high modulus of elasticity, and an exceptionally high melting point (~3000°C) [35]. Its chemical stability prevents adverse reactions with body fluids, making it suitable for long-term orthopedic implantation. Despite its favorable characteristics, the high melting point of Ta presents challenges in traditional fabrication. Early generations of synthetic implants relied on cobalt-chromium (Co–Cr) sintered beads or plasma-sprayed titanium (Ti) alloys, which suffered from poor porosity, high stiffness, and low frictional coefficients, limiting their integration with native bone [36,37]. To overcome these limitations, porous tantalum trabecular metal (PTTM) scaffolds were developed using Zimmer Biomet's Trabecular Metal™ Technology. PTTM mimics cancellous bone structurally and functionally, featuring a high-friction, low-modulus porous surface with interconnected pores and high porosity [38, 39]. Porous tantalum trabecular metal (PTTM) scaffolds exhibit a highly regular, open-cell architecture composed of repeating dodecahedral units, facilitating efficient cellular infiltration and vascularization. Fabrication typically involves pyrolysis of thermosetting polymer foams to generate a vitreous carbon template with approximately 98% porosity. Pure tantalum is then deposited onto this carbon framework via chemical vapor deposition/infiltration (CVD/CVI), resulting in a conformal tantalum coating with a typical thickness of 40–60 µm. The depth and uniformity of the coating are influenced by pore size and interconnectivity, and these structural parameters critically affect mechanical stability, load transfer capability, and cellular adhesion behavior [40, 41].

Chemical Vapor Deposition (CVD) is a key technique for fabricating high-precision porous tantalum (Ta) scaffolds. This method introduces precursor gases into a vacuum reaction chamber, which thermally decomposes or reacts with a heated substrate to deposit a solid Ta layer. By precisely controlling chamber pressure and temperature, a uniform and adherent coating forms on the scaffold template while excess gases are evacuated from the system [42]. The biological performance of CVD-fabricated porous tantalum has been validated through in vitro and in vivo studies. For instance, Hacking et al. evaluated these scaffolds in a canine spine model and observed organized fibrous tissue, enhanced bone density, and neovascularization within 4–16 weeks, demonstrating the scaffold's rapid osseointegration and mechanical stability [43]. Lu et al. explored porous cubic Ta scaffolds for lumbar interbody fusion (LIF) in rabbits, using designs with ~500 µm pores and 86.8% porosity. Energy dispersive spectroscopy confirmed material purity. BMSCs cultured on the scaffold for seven days showed excellent adhesion and proliferation, and in vivo evaluation at 12 months revealed complete

FaST - Jurnal Sains dan Teknologi, Vol. 10, No.1, Mei 2026
e-ISSN 2598-9596
DOI: https://doi.org/10.19166/fastjst.v10i1.10486
Available online at: https://ojs.uph.edu/index.php/FaSTJST/article/view/10486

histologic fusion, confirming the implant's osteoconductive potential [44]. Tanzer et al. enhanced bone formation in another study by applying low-intensity ultrasound to cylindrical porous Ta implants in canine long bones. After six weeks, stimulated implants demonstrated significantly increased bone ingrowth (8–18%) compared to controls (2.7–8.5%), highlighting the synergistic benefits of combining mechanical stimulation with porous scaffolds [45].

Bobyn et al. studied porous cylindrical Ta implants fabricated by CVD and implanted into canine bone. They utilized two pore sizes, approximately 430 µm (small) and 650 µm (large), with volume porosity between 75% and 80% and observed bone ingrowth over 52 weeks. Histologically, small-pore scaffolds achieved greater bone ingrowth at 52 weeks (95% CI 76.9–82.5%) compared to large-pore designs (95% CI 68.3–73.0%) [27]. In an earlier canine acetabular cup study, Bobyn et al. demonstrated that porous Ta (75–80%) supported higher ultimate strength relative to Co-Cr sintered-bead (~30–35%) and Ti fiber metal (~40–50%) porous coatings [46]. Higher porosity thus not only fosters cell adhesion, proliferation, and osteoblastic differentiation, but also enhances interface mechanical strength (**Fig. 3**).

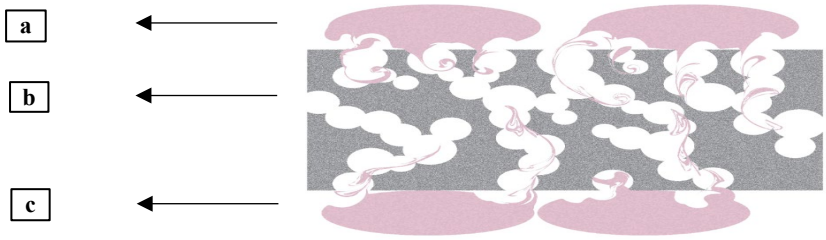

Figure 3. Process of bone in-growth into porous Ta scaffold. (a) The attachment of bone cells on the scaffold; (b) Pore size and porosity become a vital parameter to enhance bone in-growth; (c) The deep formation of bone

Kim et al. investigated the performance of porous tantalum trabecular metal (PTTM) implants compared to titanium tapered screw-vent (TSV) dental implants in a canine mandible model. Implant stability was assessed using resonance frequency analysis (RFA), yielding Implant Stability Quotient (ISQ) values ranging from 43.4 to 79.1 between 2 and 12 weeks, falling within comparable ranges for humans (50–62) and canines (59.7–89.7), with an average clinical stability threshold around 60. Histological evaluation demonstrated progressive osseointegration, evidenced by increasing bone-to-implant contact and bone ingrowth within the porous structure over the 12-week healing period. These results highlight the potential of PTTM implants to support enhanced osseointegration through bone ingrowth mechanisms during early healing [47].

Battula et al. evaluated porous tantalum trabecular metal (PTTM) and titanium tapered screw-vent (TSV) implants in a canine model, introducing ligatures after 12 weeks to induce peri-implantitis, and retrieved implants between 24 and 38 weeks [48]. Despite peri-implant inflammation, both implant designs supported tissue formation and bone healing, and there was no significant difference in tissue response between PTTM and TSV under diseased conditions. These findings suggest that implant macrodesign (porous versus threaded) does not markedly influence biological outcomes once peri-implantitis is established.

Lee et al. evaluated new bone formation in porous tantalum trabecular metal (PTTM) implants compared to titanium tapered screw-vent (TSV) dental implants in a canine mandible model [49]. Histological analysis revealed that both implant types exhibited progressive bone formation at 2 weeks and organized fibrous tissue at 12 weeks; however, PTTM demonstrated faster and more abundant bone deposition, alongside indications of ongoing remodeling, relative to TSV. These findings suggest that PTTM implants may promote enhanced osseointegration and hold promise for translation into human clinical studies.

A growing body of research supports the biocompatibility and therapeutic potential of 3D-printed porous tantalum (Ta), particularly when combined with bone marrow mesenchymal stem cells (BMMSCs). BMMSCs are a prime choice for bone tissue engineering due to their availability, ease of isolation/culture, and low immunogenicity [50]. Fu et al. demonstrated that rabbit-derived BMMSCs seeded onto porous cylindrical Ta scaffolds adhered and proliferated over seven days in vitro, and in osteonecrotic femoral models, scaffolds with BMMSCs achieved significantly superior bone formation at weeks 3 and 6 compared to scaffolds without BMMSCs [51]. Wu et al. evaluated the biocompatibility

FaST - Jurnal Sains dan Teknologi, Vol. 10, No.1, Mei 2026
e-ISSN 2598-9596
DOI: https://doi.org/10.19166/fastjst.v10i1.10486
Available online at: https://ojs.uph.edu/index.php/FaSTJST/article/view/10486

and osteoconductivity of 3D-printed porous tantalum (Ta) scaffolds implanted into the lateral epicondyle of rabbit femora. The implants featured a multiscale pore architecture, including macro-pores of 400–600 µm, interconnected micro-pores of 200–400 µm, particle sizes of 20–50 µm, and inter-particle interstices of 50–200 µm, with an overall porosity ranging from 65% to 80%. In vitro, the scaffolds supported robust cell adhesion and proliferation over eight days. Histological evaluation after 12 weeks of implantation revealed completely new bone coverage within the pores and no signs of host tissue toxicity, confirming their excellent biocompatibility and osteointegration potential [52].

Luo et al. characterized 3D-printed porous Ta implants in a rabbit femur epicondyle model, detailing a multi-scale pore structure: macro-pores of 400–600 µm, interconnected micro-pores of 200–400 µm, particle sizes of 20–50 µm, and inter-particle interstices of 50–200 µm, achieving overall porosity between 65–80%. In vitro, these scaffolds supported robust cell adhesion and proliferation over eight days, and histology at 12 weeks showed completely new bone coverage within pores, indicating no host toxicity [53]. Similarly, Wauthle et al. examined porous cylindrical Ta fabricated via selective laser melting (SLM), reporting a strut size of ~150 µm, a pore size of ~500 µm, and ≈80% porosity. Their rat femur model confirmed non-toxicity in vitro and substantial bone growth around and within the implants after 12 weeks under load-bearing conditions, demonstrating that SLM-processed Ta scaffolds support biomechanical functionality [8].

Wang et al. further demonstrated that porous Ta and Ti scaffolds with identical structures fabricated via SLM exhibited comparable osteointegration and osteogenesis. Notably, Ta scaffolds achieved mechanical properties, ultimate strength of ~394 MPa and Young's modulus of ~3.1 GPa, closely mimicking cancellous bone, alongside favorable cell performance, reinforcing the suitability of Ta for load-bearing applications [54].

In a complementary study, Balla et al. evaluated the biocompatibility of porous Ta coatings on Ti substrates fabricated using Laser Engineered Net Shaping (LENS). Human fetal osteoblasts (hFOBs) were seeded onto samples with 27% and 55% porosity. The porous Ta scaffolds, particularly those with 45% porosity and mean pore sizes exceeding 500 µm, supported robust cell adhesion and proliferation with no cytotoxic effects. In contrast, the Ti group with lower porosity (27%) showed reduced cell density. These findings suggest that porous Ta coatings significantly enhance osteoconductivity and promote superior osseointegration when processed via LENS technology [18]. Bandyopadhyay et al. observed the effects of porous Ta rods fabricated by LENS in the early osseointegration stage. The experimental design consists of three groups (Ti, Ta, Titania nanotube (TNT) with porosity of 30%) compared to dense Ti as the control, implanted in the rat distal femur model for 5 to 12 weeks. In vivo study also explained that osteoid formation was comparatively higher at 12 weeks in Ta and TNT groups, and a reduced gap width at the bone-implant interface was seen in the Ti group. A clear gap was seen in the control group, indicating Ti's poor biocompatibility. However, at five weeks, the TNT group showed comparable results to the Ta group in the early osseointegration stage. Porous Ta fabricated by LENS shows a well-ingrown bone into the implant's pores [55].

In a porcine anterior lumbar interbody fusion (ALIF) model, Zou et al. demonstrated that porous tantalum rings, filled with autograft and implanted at L2-3, L4-5, and L6-7, supported complete trabecular bone ingrowth into central holes and porous structures at 3 months, especially when combined with alendronate; carbon-fiber cages did not exhibit the same enhancement [56]. A follow-up study in the same ALIF model Zou et al. reported that bone volume and histologic fusion of Ta rings were comparable to vertebral bone and superior to carbon-fiber cages, affirming Ta's osteoconductive stability in load-bearing spinal applications [57].

Fraser et al. used a rabbit tibial gap–healing model to assess titanium implants' integration and biomechanical performance modified with a porous tantalum (Ta) midsection, compared to solid titanium controls. Implants were retrieved at 4, 8, and 12 weeks. Histomorphometric analysis showed significantly greater bone–implant contact (BIC) surrounding Ta-modified implants at all time points, and removal torque testing confirmed increased mechanical stability. Interestingly, the group's early gene expression of osteogenic markers was elevated at 4 weeks, indicating accelerated healing. In a subsequent biomechanical evaluation reported by Fraser et al., nanoindentation and resonance-frequency analyses revealed no significant differences in stiffness or hardness of the peri-implant bone–Ta interface between 4 and 12 weeks, suggesting that Ta modification enhances osteogenic response without altering the mechanical properties of the bone–implant interface [58,59].

FaST - Jurnal Sains dan Teknologi, Vol. 10, No.1, Mei 2026
e-ISSN 2598-9596
DOI: https://doi.org/10.19166/fastjst.v10i1.10486
Available online at: https://ojs.uph.edu/index.php/FaSTJST/article/view/10486

Mrosek et al. evaluated osteochondral defect repair in mature sheep using porous tantalum (PTTM) implants, both with and without an autologous periosteal graft (TMPG), compared to untreated controls. After 16 weeks, TMPG and PTTM scaffolds supported secure fixation and subchondral bone integration, exhibiting healthier neo-cartilage layers than the empty defects. Although the TMPG group demonstrated early implant stability within three months, the periosteal graft did not enhance neo-cartilage formation. In contrast, the Ta-only PTTM scaffold promoted effective bone healing in significant animal defects, highlighting its potential utility in orthopedic applications [60].

Ren et al. examined the ability of porous tantalum rods to repair tibial defects caused by firearm injuries in rabbits. Animals were divided into three groups: firearm injury with Ta implant (Group A), non-firearm injury with Ta implant (Group B), and firearm injury control (Group C). Implants were evaluated at intervals from 4 to 16 weeks. At 4 weeks, rods were covered in fibrous tissue; by 16 weeks, dense tissue fully encapsulated the implants, and radiographic scoring revealed significantly greater bone filling in Group A compared to controls, demonstrating porous Ta's effectiveness in enhancing bone healing [61].

2.3 Porous Tantalum Mechanical Properties

The mechanical performance of bone implants is strongly influenced by size, structure, architecture, and material properties, all of which modulate osseointegration. An osteoconductive surface enables bone to adhere and grow into pores, facilitating direct bone–implant contact [62]. In early healing, fibrous tissue often envelops implant surfaces, potentially infiltrating porous coatings. Studies show viable cells colonize porous Ta, consistent with osteoconductive behavior [63]. The mechanical properties of porous Ta are also critical: while bulk Ta has an elastic modulus of ~185 GPa, porosity reduces this to approximately 3 GPa, closer to human cancellous bone (cortical bone is ~20 GPa), minimizing stress shielding [64]. With advanced manufacturing and CAD design, 3D-printed porous Ta scaffolds can achieve tailored pore architecture and mechanical functionality for long-term load-bearing applications.

Zardiackas et al. found that porous tantalum foam (Hedrocel™) exhibited significantly higher cantilever bending strength (110 ± 14 MPa), compressive strength (~60 MPa), and tensile strength (~63 MPa) compared to cancellous bone. Its fatigue endurance limits (23 MPa in compression and 35 MPa in bending at 5×10^6 cycles) also surpassed those of both cancellous and cortical bone. These robust mechanical properties, alongside its known biocompatibility, underscore the suitability of porous Ta foam for load-bearing orthopedic implants [38]. Hacking et al. investigated the biomechanical strength and histological progression of soft tissue ingrowth into porous tantalum implants in a canine model. Peel tests at 4, 8, and 16 weeks revealed mean soft tissue attachment strengths of 61 ± 37 g/mm, 71 ± 38 g/mm, and 89 ± 43 g/mm, respectively, indicating statistically normal distributions and rapid integration. Histological analyses demonstrated mature, vascularized fibrous tissue formation within the porous structure, which increased in density over time, signifying progressive healing and improved interface bonding [43].

Porous tantalum scaffolds are designed to replicate the mechanical properties of cancellous bone, offering a tangent elastic modulus in the range of 2–3 GPa, comparable to human cancellous bone, while maintaining an optimal balance between stiffness and biological function [65,66]. This reduced modulus helps mitigate stress shielding risks while providing sufficient load-bearing capacity for bone ingrowth and graft stability. That balance is critical: an implant that is too compliant may risk structural failure, whereas an overly stiff device can lead to bone resorption and implant loosening due to stress shielding [67] and the general physical properties of pure tantalum showed in (**Table 3**) [68,69]

Table 3 General physical properties of pure tantalum [70,71]

Indicators	Value
Elastic modulus	185 GPa
Yield strength	165 MPa
Elongation to failure	40%
Tensile strength	205 MPa
Density	16.9 g/cm^3
Melting points	3000 ^{o}C
Hardness (HV)	110

FaST - Jurnal Sains dan Teknologi, Vol. 10, No.1, Mei 2026
e-ISSN 2598-9596
DOI: https://doi.org/10.19166/fastjst.v10i1.10486
Available online at: https://ojs.uph.edu/index.php/FaSTJST/article/view/10486

Wauthle et al. investigated the mechanical testing of static and dynamic porous Ta fabricated by SLM. Based on the experiment, the actual static mechanical properties of porous Ta with a yield strength of 12.7 ± 0.6 MPa and elastic modulus of 1.22 ± 0.07 GPa are close to the range of human cancellous bone. However, these results have a lower modulus value and could lower the stress-shielding effects. In ex vivo testing (torsion), two out of five explants have a robust bone interface to repair the bone defect with maximum torque (450 Nmm) applied. The maximum torque (331.3 Nmm) and average rotation of 59.1 ° were applied to three failed explants. The results did not significantly indicate that the bone-implant interface was as strong as the host bone. The porous Ta has good fatigue behavior, as shown by its high ductility properties and fatigue limit of 7.45 MPa, which is relatively high resistance. Thus, porous Ta's fabrication by the SLM technology performs excellent osteoconductive properties and is considered for serial manufacturing implants in comprehensive orthopedic research [8].

Guo et al. compared 3D-printed porous tantalum (Ta) scaffolds fabricated via selective laser melting (SLM) with Ti6Al4V controls. Both had a 300–400 μm pore size and 80% porosity and were implanted into rabbit femoral defects. In vitro, human bone marrow mesenchymal stem cells (hBMSCs) exhibited superior adhesion and full spread on Ta scaffolds after seven days. In vivo, at 12 weeks, Ta scaffolds showed significantly greater new bone area and thickness than Ti6Al4V implants, confirming Ta's effective osteogenesis and osseointegration [70]. SLM-fabricated porous tantalum scaffolds have a compressive strength of 78.54 MPa compared to 71.04 MPa for porous Ti6Al4V, and elastic moduli of 2.34 GPa versus 2.27 GPa, respectively. These values closely mimic human cancellous bone and help reduce stress shielding by matching physiological stiffness [70].

Blanco et al. investigated the in vitro proliferation of bone marrow-derived mesenchymal stem cells (BMSCs) co-cultured on porous titanium (Ti) and tantalum (Ta) scaffolds for inter-somatic spinal fusion. Over 14 days, BMSCs adhered and proliferated on both scaffold types, with a slightly higher proliferation rate observed in the Ti group. Nevertheless, the porous Ta scaffold exhibited comparable biocompatibility, demonstrating its ability to support cell attachment and growth. Although the study could not quantify the exact number of cells adhering to each scaffold, both materials showed promise for spinal fusion or reconstructive applications, highlighting Ta's potential in clinical settings [71].

Han Wang et al. compared the static mechanical properties of additively manufactured porous tantalum (Ta) and titanium (Ti) scaffolds fabricated via selective laser melting (SLM). They found that porous Ti exhibited a significantly higher equivalent stress (393.6 ± 1.4 MPa) compared to porous Ta (139.8 ± 14.5 MPa; $p < .05$). Additionally, the Young's modulus of the Ta group (3.10 ± 0.03 GPa) was significantly lower than that of Ti (5.42 ± 0.07 GPa; $p < .05$), aligning Ta's stiffness more closely with that of cancellous bone. Push-out tests conducted at 2-, 4-, and 8-weeks post-implantation revealed similar peak bone–implant bonding strength in both groups. However, the Ta implants showed lower displacement under load, suggesting better damping and cushioning, while Ti displayed higher microhardness. Overall, porous Ta scaffolds exhibit a favorable combination of mechanical compatibility and bone integration for long-term use [72].

Balla et al. evaluated the mechanical properties of porous Ta fabricated by LENS technology. The porous Ta has an open pore volume, with the microstructure appearing to vary in pore size and interconnectivity. Then, the 0.2% proof strength and Young modulus elasticity show a function of relative density. 0.2% proof strength ranges from 100 to 746 MPa, while Young's modulus is 1.5 to 20 GPa. These mechanical properties are similar to human cortical bone [18]. Bandyopadhyay et al. performed push-out testing in porous Ta fabricated by LENS to evaluate the bone-material interlocking interface. Field emission scanning electron microscopy (FESEM) analysis assessed the bone-implant interface's morphological characteristics. The FESEM micrograph at five and twelve weeks shows that volume fraction porosity plays a crucial role in the early stage of osteointegration. The porous Ta with a porosity of 30 % shows a well-ingrown bone at five weeks of implantation that demonstrates bone-material interlocking. However, when the push-out was performed, the broken bone material indicates that the mechanical properties were similar, if not more substantial, than the bone's strength [58].

Wei et al. developed a biphasic construct combining porous tantalum (pTa) fabricated via chemical vapor deposition (CVD) and a 3D collagen membrane (3D CM), each seeded with BMSCs or chondrocytes, for repairing large goat femoral osteochondral defects. Mechanical evaluation revealed a compressive strength of 43.04 MPa for pTa and 3.40 MPa for 3D CM, with tensile and shear strengths also measured at the pTa–CM interface using porcine fibrin sealant. The study further confirmed that

FaST - Jurnal Sains dan Teknologi, Vol. 10, No.1, Mei 2026
e-ISSN 2598-9596
DOI: https://doi.org/10.19166/fastjst.v10i1.10486
Available online at: https://ojs.uph.edu/index.php/FaSTJST/article/view/10486

porous Ta's elastic modulus sits between the cortical and cancellous bone range, conducive to bone remodeling, without impeding mechanical performance or cell viability [73].

2.4 Molecular Mechanisms (MAPK/ERK, Macrophage polarization, BMP signaling)

Additive manufacturing (AM), fabricated porous tantalum (pTa) scaffolds are engineered to harmonize mechanical strength with biological activity, supporting cell attachment, proliferation, and osseointegration. These scaffolds, designed with precise pore architecture, have consistently demonstrated excellent biocompatibility and non-toxicity in both in vitro and in vivo settings [74]. The surface properties, including micro- and nano-scale topography and hydrophilicity, play a critical role in initial cell adhesion; scaffold modifications with bioactive coatings, such as peptides or extracellular matrix molecules, further facilitate this attachment and subsequent cell growth. Incorporating osteoconductive agents such as bone morphogenetic proteins (BMPs) or growth factors into the scaffold matrix has been shown to stimulate osteogenesis and vascularization, enhancing graft integration and bone regeneration in both laboratory and animal models [75].

Zhou et al. reported that mesenchymal stem cell (MSC)-seeded porous tantalum scaffolds demonstrate considerable potential for bone regeneration due to their favorable mechanical properties, biocompatibility, and capacity to support MSC adhesion, proliferation, and osteogenic differentiation. The synergistic interaction between scaffold architecture and cellular activity suggests translational relevance for bone tissue engineering and orthopedic reconstruction, particularly in the management of complex defects and degenerative bone conditions. Quantitative assessments, including MTT assays, alkaline phosphatase (ALP) activity, calcium deposition analysis, bone volume fraction (BV/TV), and push-out mechanical testing, consistently indicate enhanced osteogenesis and improved interfacial integration when porous tantalum is combined with MSCs.[76].

An inflammatory microenvironment orchestrated by macrophages is pivotal to bone repair. Sun et al. demonstrated that tantalum nanoparticles (TaNPs) are non-cytotoxic to RAW 264.7 macrophages, which can effectively phagocytose these particles without compromising viability. Moreover, TaNPs (5 μg/mL) suppressed the expression of pro-inflammatory genes (IL-1β, IL-18, TNF-α, iNOS) and induced anti-inflammatory markers (IL-10, TGF-β1, VEGFA) under LPS and IFN-γ stimulation. The study also observed increased M2-like polarization and reduced intracellular ROS, suggesting that TaNPs promote a reparative macrophage phenotype and regulate immune responses, beneficial for bone regeneration [77].

Porous tantalum (Ta) scaffolds functionalized with bone morphogenetic protein-7 (BMP-7) have shown enhanced osteochondral repair in preclinical models. Wang et al. developed a porous Ta rod loaded with BMP-7 and implanted it into rabbit medial femoral condyle osteochondral defects. Histological analysis at 16 weeks post-operation revealed significantly greater regeneration of both subchondral bone and cartilage, fibrocartilage and fibrous tissue, compared to unmodified Ta implants and empty controls. Micro-CT and biomechanical testing confirmed increased bone volume fraction and superior interface strength in the BMP-7-modified group. These results support combining osteo-inductive factors like BMP-7 with porous Ta scaffolds to stimulate MSC differentiation and improve graft integration in bone repair [78].

In a porcine ALIF model, Huang et al. evaluated porous tantalum (Ta) pedicle-screw implants and carbon-fiber cages, both with and without concurrent alendronate (ALN) administration. Histological analysis at 3 months revealed that Ta implants, particularly those with pedicle screw fixation, achieved improved bone ingrowth and fusion strength. Animals treated with ALN showed notably greater bone volume in the Ta implant's central hole and porous structure than untreated counterparts, while fibrous tissue presence remained comparable. Importantly, long-term ALN withdrawal did not sustain enhanced bone ingrowth, indicating that its benefits are limited to the early post-operative phase [79].

Dou et al. investigated the molecular mechanism by which porous tantalum (pTa) scaffolds promote osteogenic differentiation of bone marrow mesenchymal stem cells (BMMSCs). They demonstrated that BMMSCs cultured on pTa exhibited significantly higher mRNA expression of osteogenic markers, osterix (OSX), collagen I (COL-I), osteonectin (OSN), and osteocalcin (OCN), compared to titanium controls. This upregulation was accompanied by increased phosphorylation of ERK, indicating activation of the MAPK/ERK signaling cascade. Notably, inhibition of ERK using

FaST - Jurnal Sains dan Teknologi, Vol. 10, No.1, Mei 2026
e-ISSN 2598-9596
DOI: https://doi.org/10.19166/fastjst.v10i1.10486
Available online at: https://ojs.uph.edu/index.php/FaSTJST/article/view/10486

U0126 attenuated both ERK phosphorylation and the elevated expression of osteogenic genes, confirming that pTa induces osteogenesis through the MAPK/ERK pathway in vitro [80].

Guo et al. investigated the osteogenic potential of 3D-printed porous tantalum scaffolds versus porous Ti6Al4V scaffolds using human bone marrow–derived mesenchymal stem cells (hBMSCs). They found significantly enhanced expression of early osteogenic markers, RUNX2, ALP, and COL1, in the Ta group compared to Ti and controls. Late markers OCN and OPN were similar on day 7 but showed elevated levels in the Ta group on day 14, indicating sustained osteogenic differentiation promoted by porous tantalum scaffolds [54].

2.5 Clinical Evidence of Porous Tantalum Application in Medical

Beyond experimental and preclinical investigations, porous tantalum has demonstrated substantial clinical applicability across multiple orthopedic and dental indications. Its high porosity, interconnected architecture, and favorable elastic modulus enable enhanced mechanical interlocking, bone in-growth, and long-term implant stability in load-bearing environments. Accumulating clinical evidence from dental implants, hip arthroplasty, osteonecrosis management, and knee revision procedures underscores the translational potential of porous tantalum-based devices. The following sections summarize representative clinical outcomes across major application domains, highlighting functional recovery, implant survivorship, and radiographic evidence of osseointegration.

2.5.1 Dental Surgery Application

The clinical application of porous tantalum trabecular metal (PTTM) in dental implants has expanded significantly. PTTM-enhanced titanium implants offer superior osseointegration and are increasingly preferred for immediate placement procedures over conventional dental implants. In a rabbit femoral condyle model, Al Deeb et al. reported that PTTM-enhanced implants achieved significantly higher bone-to-implant contact (BIC: $57.9 \pm 6.5\%$ vs. $47.6 \pm 8.0\%$) and increased peri-implant bone volume compared to traditional titanium screws ($p < 0.05$) [81]. Additionally, Cui et al., study using vacuum plasma-sprayed micro-nano porous Ta–coated Ti implants found that the Ta coating enhanced hydrophilicity, protein adsorption, and mesenchymal stem cell activity, while canine mandible implants showed increased bone mineral density and new bone formation [82]. These recent findings confirm that PTTM modifications improve implant osseointegration and mechanical stability. Such advances support the use of PTTM implants, especially for immediate dental applications and in patients with high clinical risks or compromised sites.

Edelmann et al. conducted a retrospective analysis comparing porous tantalum trabecular metal (PTTM) implants to Tapered Screw-Vent (TSV) titanium implants, both used with and without demineralized bone matrix (DBM), for immediate post-extraction dental placement. The study found that PTTM implants combined with DBM had a significantly lower risk of peri-implant bone loss and a higher probability of bone gain after one year, compared to their TSV counterparts. This suggests incorporating DBM with PTTM implants provides a bone-preserving strategy equivalent to autografts for immediate placement protocols [83].

Bencharit et al. compared porous tantalum trabecular metal (PTTM) implants to titanium alloy implants during early wound healing in the human oral cavity. In a split-mouth design involving 12 patients, one PTTM and one Ti implant were placed in the mandible. Biopsies taken in two weeks showed significantly higher expression of neovascularization, wound healing, and osteogenesis genes, including BMPs, collagens, and growth factors in the PTTM group compared to the Ti controls. Histological analysis for four weeks revealed greater bone infiltration and vascularization around PTTM surfaces. These findings suggest that PTTM implants enhance early bone ingrowth and vascularization, leading to faster and more robust bone healing than standard titanium implants [84].

2.5.2 Hip-Joint Implant Application

Unger et al. evaluated the performance of a trabecular metal (TM) monoblock acetabular cup in revision total hip arthroplasty (THA). In a cohort of 60 patients with prior acetabular component failure, followed by an average of 42 months, radiographs showed full graft incorporation and no postoperative infection or aseptic loosening cases. Harris Hip Scores improved significantly from a preoperative average of 74.8 to 94.4 at final follow-up, indicating excellent implant stability and bone ingrowth facilitated by

FaST - Jurnal Sains dan Teknologi, Vol. 10, No.1, Mei 2026
e-ISSN 2598-9596
DOI: https://doi.org/10.19166/fastjst.v10i1.10486
Available online at: https://ojs.uph.edu/index.php/FaSTJST/article/view/10486

TM implants' high friction coefficient and porous architecture [85]. Haidemenopoulos et al. conducted a histological analysis of a retrieved porous tantalum (Ta) monoblock acetabular cup removed four years post-implantation in a female THA patient. Using optical and scanning electron microscopy, they observed gradual human bone ingrowth into the first two rows of porous cells, reaching a depth of approximately 1.5–2 mm, with bone deposition directly on Ta struts and progressive densification into hydroxyapatite as evidenced by matching Ca:P ratios [86]. Moen et al. performed a radiographic evaluation of 51 THA patients with implanted porous Ta monoblock cups. At an average follow-up of 10.3 years, helical CT scans with metal suppression protocols revealed no signs of periprosthetic osteolysis in the pelvis or proximal femur. This suggests that the monoblock porous architecture may reduce osteolytic risk compared to conventional designs [87]. Tsao et al. do not apply to femoral head implants. Instead, current evidence shows that modern porous Ta rods, such as Runze- or AM-fabricated TaBw01 devices, offer excellent mechanical stability in ONFH. Clinical implants demonstrate no radiographic signs of loosening or radiolucency, and their elastic modulus is well-matched to native bone, providing initial fixation and long-term integration [88].

In early-stage osteonecrosis of the femoral head (ARCO I–II), implantation of porous tantalum rods has shown promising results. Huang et al. compared a newly developed Runze porous Ta rod to a standard Zimmer Ta implant in a cohort study with at least three years of follow-up, reporting comparable improvements in Harris Hip Scores and demonstrating substantial bone ingrowth into the rod's porous architecture [89]. Similarly, Zhang et al. analyzed outcomes in 86 ARCO II patients. They concluded that mechanical stability depends heavily on precise implant alignment and rod length, noting that optimized placement enhances long-term graft support [90].

In a clinical study by Zhao et al., the authors evaluated a novel technique that combined autologous bone marrow mesenchymal stem cells (BMMSCs) with porous tantalum rod implantation and vascularized iliac bone grafting to treat end-stage osteonecrosis of the femoral head (ARCO IIIc–IV). Over a mean follow-up of 64 months, the joint-preserving surgery resulted in a success rate of 89.5% for stage IIIc hips and 75% for stage IV hips, significantly reducing the need for total hip arthroplasty. Harris Hip Scores improved markedly from 38.7 preoperatively to 77.2 postoperatively, demonstrating both safety and effective restoration of hip function in end-stage ONFH patients [91].

2.5.3 Knee Implant Application

A multicenter retrospective cohort study by Kayani et al. (2024) followed 152 patients who underwent revision TKA using porous Ta metaphyseal cones (mean follow-up: 5.6 years). This study, including cases of aseptic loosening and infection, reported 100% cone survival (no revisions of cones themselves) and 83.8% overall implant survival, with consistent radiographic evidence of osseointegration and satisfactory functional scores [92].

Hadley et al. conducted a single-center study involving 228 revision TKAs with tibial Ta cones, reporting 97% survivorship free of aseptic cone removal and 88% overall cone survival at a mean follow-up of 6.3 years (range 5–10 years). Only minor radiolucencies appeared in <5% of cases, suggesting durable fixation and bone ingrowth [93].

A 2024 finite-element analysis by Piovan et al. alongside preliminary clinical data showed that 3D-printed patient-specific metaphyseal Ta cones achieved favorable load distribution and stress stability, suggesting superior biomechanical performance compared to traditional stems [94].

Mao et al. researched a patient-specific 3D-printed porous tantalum (Ta) prosthesis for knee joint revision surgery in an 84-year-old man, using experimental mechanical testing and finite element analysis (FEA) derived from patient CT data, a novel methodology in clinical practice. By conducting mechanical tests on several pore and wire combinations produced using selective laser melting (SLM), the researchers determined the ideal design (600 μm pore, 900 μm wire), which resulted in a Young's modulus of 5.72 GPa and a yield strength of 172 MPa. This design satisfied all mechanical and biomechanical safety standards, with prosthesis strength surpassing load stress, tibial strain within the optimal range of 400–3,000 με, and tibial stress remaining below 60 MPa. Following implantation in 2017, a five-year follow-up demonstrated exceptional bone-prosthesis integration and complete patient recovery. This research creates a clinically proven framework for biomechanical matching using CT-based design optimization and finite element analysis, establishing new benchmarks for individualized orthopedic implants. It underscores the need for future models to combine anisotropic bone

FaST - Jurnal Sains dan Teknologi, Vol. 10, No.1, Mei 2026
e-ISSN 2598-9596
DOI: https://doi.org/10.19166/fastjst.v10i1.10486
Available online at: https://ojs.uph.edu/index.php/FaSTJST/article/view/10486

characteristics and localized bone density to improve mechanical precision, thereby promoting individualized, load-bearing, and physiologically integrated approaches in revision arthroplasty [95].

3. MSC-driven bone generation using 3D printed Tantalum Scaffolds

Integrating mesenchymal stem cells (MSCs) with 3D-printed porous tantalum (PTa) scaffolds has become a practical approach for promoting bone regeneration. Recent studies have concentrated on augmenting these scaffolds using bioactive surface changes, nano-topography, and biological agents to enhance MSC adhesion, differentiation, and in vivo bone formation. The following table juxtaposes five recent experiments, emphasizing critical manufacturing techniques, MSC integration, scaffold improvements, assessment models, and results. The comparative study showed in **Table 4** that nano-topography of PTa significantly enhanced BMSC adhesion, as reported by Zhang et al. (2023) [96]. Liu et al also reported that porous pTa promoted M2 macrophage shift, inhibited inflammation, and enhanced BMSC osteogenesis via P38-MAPK [97]. Jiao et al. also state that 70–80% porosity of PTa provided maximal BMSC proliferation, osteogenic gene expression, and bone ingrowth; 70% porosity was optimal [98]. Yu et al.confirmed a review of customized PTa high BMSC proliferation, osteogenesis, corrosion resistance, and overall biocompatibility [99]. Zhao et al. reported that porous Ta promoted osteogenesis and angiogenesis, indicating vascularized bone regeneration [100].

Table 4 Comparative Study of Recent Studies of 3D-Printed Porous Tantalum

Study	Fabrication	MSC Integration	Scaffold Modification	Model	Results
Zhang et al. (2023) [96]	SLM-printed PTa with hydrothermal nano-topography	Rat BMSCs (in vitro)	Nano-structured surface via alkali–heat–hydrothermal treatment	Rabbit mandibular defect (in vivo)	Nano-topography significantly enhanced BMSC adhesion, osteogenic differentiation (↑ALP, mineralization), and early bone formation.
Liu et al. (2025) [97]	3D-printed PTa with polydopamine; MZIF-8 drug delivery	BMSC regulation via macrophage polarization	Polydopamine + MZIF-8 + melatonin for immunoregulatory release	Osteoporotic rat femur (in vivo)	Promoted M2 macrophage shift, inhibited inflammation, enhanced BMSC osteogenesis via P38-MAPK
Jiao et al. (2023) [98]	SLM-printed PTa scaffolds (60%, 70%, 80% porosity)	Rat BMSCs (in vitro)	Varying porosity only	Rat femoral defect (in vivo)	70–80% porosity provided maximal BMSC proliferation, osteogenic gene expression, and bone ingrowth; 70% porosity was optimal
Yu et al. (2024) [99]	SLM-printed PTa with corrosion-resistant surface	Human BMSCs (in vitro)	Review of customized PTa (no specific coating)	-	Confirmed high BMSC proliferation, osteogenesis, corrosion resistance, and overall biocompatibility
Zhao et al. (2025) [100]	Porous Ta integrated with gelatin nanoparticle (GNP) hydrogel	BMSC + endothelial co-culture	GNP hydrogel for growth factor delivery and angiogenesis	In vivo vascularized bone model	Promoted both osteogenesis and angiogenesis, indicating vascularized bone regeneration

4. Conclusions and Future Directions

Three-dimensional (3D)-printed porous tantalum (Ta) scaffolds represent a significant advancement in musculoskeletal tissue engineering. Their favorable mechanical compatibility, corrosion resistance, and high biocompatibility provide an effective platform for supporting bone ingrowth and long-term osseointegration. Additive manufacturing technologies, including selective laser melting and laser-

engineered net shaping, enable precise control of pore size, porosity, and internal architecture, allowing the fabrication of scaffolds that closely mimic native bone structure and mechanical behavior.

The incorporation of bone marrow–derived mesenchymal stem cells (BMSCs) further enhances the regenerative capacity of porous Ta constructs by promoting osteogenic differentiation, extracellular matrix deposition, and mineralization. Emerging translational studies indicate that patient-specific porous Ta implants designed using biomechanical modeling and finite element analysis demonstrate promising mid-term clinical outcomes, reinforcing the clinical feasibility of personalized scaffold strategies.

Future research should prioritize optimization of graded pore architectures to better replicate cortical–cancellous transitions, alongside long-term in vivo evaluation of remodeling, vascularization, and fatigue resistance under physiological loading conditions. Standardization of scaffold design parameters, manufacturing reproducibility, and regulatory pathways will be critical for accelerating broader clinical adoption. Additionally, integrating immunomodulatory strategies and coupled osteogenic–angiogenic approaches may further enhance therapeutic outcomes for complex bone defects.

Despite continued challenges, including manufacturing scalability and limited long-term randomized clinical data, the convergence of advanced additive manufacturing, regenerative cell therapy, and biomechanical optimization positions porous tantalum scaffolds as a promising strategy for next-generation orthopedic reconstruction.

5. Policy on the Use of Generative Artificial Intelligence (AI)

Generative artificial intelligence (ChatGPT, OpenAI) was used solely for language editing and clarity improvement. The authors take full responsibility for the originality, accuracy, and integrity of the content of this manuscript.

Acknowledgement

M.L. conducted the comprehensive literature review, prepared all graphical illustrations using Adobe Illustrator®, interpreted the data, and drafted the manuscript. All co-authors contributed to critical revision of the intellectual content and approved the final version prior to submission. M.X.S. provided overall supervision and guidance throughout the study.

Strength of the Study

This review provides a comprehensive and integrative synthesis of 3D-printed porous tantalum (Ta) scaffolds by systematically linking scaffold design parameters, additive manufacturing techniques, mechanical performance, biological mechanisms, and clinical outcomes. Unlike prior reviews that primarily focus on titanium-based biomaterials or broadly discuss metallic scaffolds, this study specifically centers on porous Ta and consolidates interdisciplinary evidence spanning material science, mechanobiology, molecular signaling pathways, and long-term clinical follow-up data.

A key strength lies in the integration of mechanical benchmarks with cellular, osteogenic, and immunomodulatory pathways, thereby bridging fundamental laboratory research with translational orthopedic applications. By contextualizing scaffold architecture within both biomechanical requirements and biological responses, this review offers a clinically oriented framework that supports patient-specific implant design and future precision-based bone repair strategies.

Limitation of the Study

Several limitations should be acknowledged. First, as a narrative review, the study does not employ a formal systematic review protocol or meta-analytic approach; therefore, selection bias cannot be entirely excluded. Although efforts were made to prioritize methodological rigor and thematic relevance, the absence of quantitative synthesis limits direct statistical comparability across studies.

Second, substantial heterogeneity exists among the included studies with respect to scaffold architecture, pore geometry, additive manufacturing platforms, animal models, mesenchymal stem cell sources, and outcome assessment methods. This variability restricts direct quantitative comparison of mechanical and biological outcomes.

Third, although preclinical evidence is extensive, long-term human clinical studies, particularly

large-scale randomized controlled trials, remain limited. In addition, manufacturing variability across additive platforms may influence reported mechanical properties and biological performance, potentially affecting reproducibility and translational standardization.

Future systematic analyses and standardized reporting frameworks are warranted to strengthen evidence comparability and accelerate clinical translation.

Figure Preparation and Copyright Statement

All schematic illustrations (Figures 1–3) were independently developed by the authors using Adobe Illustrator® based on synthesized concepts derived from the reviewed literature. No previously published copyrighted images were reproduced. Where conceptual elements were adapted from existing studies, appropriate citations have been provided in the corresponding figure legends.

References

[1] Fernandez-Fairen, M., Querales, V., Jakowlew, A., Torres, A., Murcia, A., & Gil-Garay, E. (2010). Tantalum is a good bone graft substitute in tibial tubercle advancement. *Clinical Orthopaedics and Related Research*, *468*(5), 1284–1295. https://doi.org/10.1007/s11999-009-1115-0

[2] Huang, G., Pan, S.-T., & Qiu, J.-X. (2021). The clinical application of porous tantalum and its new development for bone tissue engineering. *Materials*, *14*(10), 2647. https://doi.org/10.3390/ma14102647

[3] Ni, J., Ling, H., Zhang, S., Wang, Z., Peng, Z., Benyshek, C., Zan, R., Miri, A. K., Li, Z., Zhang, X., Lee, J., Lee, K. J., Kim, H. J., Tebon, P., Hoffman, T., Dokmeci, M. R., Ashammakhi, N., Li, X., & Khademhosseini, A. (2019). Three-dimensional printing of metals for biomedical applications. *Materials today. Bio*, *3*, 100024. https://doi.org/10.1016/j.mtbio.2019.100024

[4] Hadjidakis, D. J., & Androulakis, I. I. (2006). Bone remodeling. *Annals of the New York Academy of Sciences*, *1092*, 385–396. https://doi.org/10.1196/annals.1365.035

[5] Arias, C. F., Herrero, M. A., Echeverri, L. F., Oleaga, G. E., & López, J. M. (2018). Bone remodeling: A tissue-level process emerging from cell-level molecular algorithms. *PloS one*, *13*(9), e0204171. https://doi.org/10.1371/journal.pone.0204171

[6] Florencio-Silva, R., Sasso, G. R., Sasso-Cerri, E., Simões, M. J., & Cerri, P. S. (2015). Biology of Bone Tissue: Structure, Function, and Factors That Influence Bone Cells. *BioMed research international*, *2015*, 421746. https://doi.org/10.1155/2015/421746

[7] Torres, Y., Lascano, S., Bris, J., Pavón, J., & Rodriguez, J. A. (2014). Development of porous titanium for biomedical applications: A comparison between loose sintering and space-holder techniques. *Materials Science and Engineering: C*, *44*, 330–334. https://doi.org/10.1016/j.msec.2013.11.036

[8] Wauthle, R., van der Stok, J., Amin Yavari, S., Van Humbeeck, J., Kruth, J. P., Zadpoor, A. A., Weinans, H., Mulier, M., & Schrooten, J. (2015). Additively manufactured porous tantalum implants. *Acta biomaterialia*, *14*, 217–225. https://doi.org/10.1016/j.actbio.2014.12.003

[9] Kruth, J. P., Levy, G., Klocke, F., & Childs, T. H. C. (2007). Consolidation phenomena in laser and powder-bed based layered manufacturing. *CIRP Annals - Manufacturing Technology*, *56*(2), 730–759. https://doi.org/10.1016/j.cirp.2007.10.004

[10] Izadi, M., Farzaneh, A., Mohammed, M., Gibson, I., & Rolfe, B. (2020). A review of laser engineered net shaping (LENS) build and process parameters of metallic parts. *Rapid prototyping journal*, *26*(6), 1059-1078. https://doi.org/10.1108/RPJ-04-2018-0088

[11] Kapat, K., Srivas, P. K., Rameshbabu, A. P., Maity, P. P., Jana, S., Dutta, J., Majumdar, P., Chakrabarti, D., & Dhara, S. (2017). Influence of Porosity and Pore-Size Distribution in Ti6Al4 V Foam on Physicomechanical Properties, Osteogenesis, and Quantitative Validation of Bone Ingrowth by Micro-Computed Tomography. *ACS applied materials & interfaces*, *9*(45), 39235–39248. https://doi.org/10.1021/acsami.7b13960

[12] Dejene, N. D., & Lemu, H. G. (2023). Current status and challenges of powder bed fusion-based metal additive manufacturing: Literature review. *Metals, 13*(2), 424. https://doi.org/10.3390/met13020424

[13] Wu, Y., Lu, Y., Zhao, M., Bosiakov, S., & Li, L. (2022). A critical review of additive manufacturing techniques and associated biomaterials used in bone tissue engineering. *Polymers*, *14*(10), 2117. https://doi.org/10.3390/polym14102117

[14] Hu, D., & Kovacevic, R. (2003). Sensing, modeling and control for laser based additive manufacturing. *International Journal of Machine Tools and Manufacture*, *43*(1), 51–60. https://doi.org/10.1016/S0890-6955(02)00163-3

[15] Yap, C. Y., Chua, C. K., Dong, Z. L., Liu, Z. H., Zhang, D. Q., Loh, L. E., & Sing, S. L. (2015). Review of selective laser melting: Materials and applications. *Applied Physics Reviews*, *2*(4), 041101. https://doi.org/10.1063/1.4935926
[16] Balla, V. K., Banerjee, S., Bose, S., & Bandyopadhyay, A. (2010). Direct laser processing of a tantalum coating on titanium for bone replacement structures. *Acta Biomaterialia, 6*(6), 2329–2334. https://doi.org/10.1016/j.actbio.2009.11.021
[17] Hussein, K. H., Park, K. M., Kang, K. S., & Woo, H. M. (2016). Biocompatibility evaluation of tissue-engineered decellularized scaffolds for biomedical application. *Materials Science and Engineering: C, 67*, 766–778. https://doi.org/10.1016/j.msec.2016.05.068
[18] Gibson, I., Rosen, D. W., & Stucker, B. (2020). *Additive manufacturing technologies* (3rd ed.). Springer. https://doi.org/10.1007/978-3-030-56127-7
[19] Wang, Z., Wang, C., Li, C., Qin, Y., Zhong, L., Chen, B., Li, Z., Liu, H., Chang, F., & Wang, J. (2017). Analysis of factors influencing bone ingrowth into three-dimensional printed porous metal scaffolds: A review. *Journal of Alloys and Compounds*, *717*, 271–285. https://doi.org/10.1016/j.jallcom.2017.05.079
[20] Matena, J., Petersen, S., Gieseke, M., Kampmann, A., Teske, M., Beyerbach, M., Murua Escobar, H., Haferkamp, H., Gellrich, N.-C., & Nolte, I. (2015). SLM produced porous titanium implant improvements for enhanced vascularization and osteoblast seeding. *International Journal of Molecular Sciences, 16*(4), 7478–7492. https://doi.org/10.3390/ijms16047478
[21] Hulbert, S. F., Young, F. A., Mathews, R. S., Klawitter, J. J., Talbert, C. D., & Stelling, F. H. (1970). Potential of ceramic materials as permanently implantable skeletal prostheses. *Journal of Biomedical Materials Research*, *4*(3), 433–456. https://doi.org/10.1002/jbm.820040309
[22] Cheng, A., Humayun, A., Cohen, D. J., Boyan, B. D., & Schwartz, Z. (2014). Additively manufactured 3D porous Ti-6Al-4V constructs mimic trabecular bone structure and regulate osteoblast proliferation, differentiation and local factor production in a porosity and surface roughness dependent manner. *Biofabrication*, *6*(4), 045007. https://doi.org/10.1088/1758-5082/6/4/045007
[23] Biemond, J. E., Aquarius, R., Verdonschot, N., & Buma, P. (2011). Frictional and bone ingrowth properties of engineered surface topographies produced by electron beam technology. *Archives of Orthopaedic and Trauma Surgery*, *131*(5), 711–718. https://doi.org/10.1007/s00402-010-1218-9
[24] Vaiani, L., Boccaccio, A., Uva, A. E., Palumbo, G., Piccininni, A., Guglielmi, P., Cantore, S., Santacroce, L., Charitos, I. A., & Ballini, A. (2023). Ceramic Materials for Biomedical Applications: An Overview on Properties and Fabrication Processes. *Journal of functional biomaterials*, *14*(3), 146. https://doi.org/10.3390/jfb14030146
[25] Otsuki, B., Takemoto, M., Fujibayashi, S., Neo, M., Kokubo, T., & Nakamura, T. (2006). Pore throat size and connectivity determine bone and tissue ingrowth into porous implants: Three-dimensional micro-CT based structural analyses of porous bioactive titanium implants. *Biomaterials*, *27*(35), 5892–5900. https://doi.org/10.1016/j.biomaterials.2006.08.013
[26] Prananingrum, W., Naito, Y., Galli, S., Bae, J., Sekine, K., Hamada, K., Tomotake, Y., Wennerberg, A., Jimbo, R., & Ichikawa, T. (2016). Bone ingrowth of various porous titanium scaffolds produced by a moldless and space holder technique: An in vivo study in rabbits. *Biomedical Materials*, *11*(1), 015012. https://doi.org/10.1088/1748-6041/11/1/015012
[27] Bobyn, J. D., Stackpool, G. J., Hacking, S. A., Tanzer, M., & Krygier, J. J. (1999). Characteristics of bone ingrowth and interface mechanics of a new porous tantalum biomaterial. *Journal of Bone and Joint Surgery - British Volume*, *81*(5), 907–914. https://doi.org/10.1302/0301-620x.81b5.9283
[28] Li, J. P., Habibovic, P., van den Doel, M., Wilson, C. E., de Wijn, J. R., van Blitterswijk, C. A., & de Groot, K. (2007). Bone ingrowth in porous titanium implants produced by 3D fiber deposition. *Biomaterials*, *28*(18), 2810–2820. https://doi.org/10.1016/j.biomaterials.2007.02.020
[29] Navarro, M., Michiardi, A., Castaño, O., & Planell, J. A. (2008). Biomaterials in orthopaedics. *Journal of the Royal Society Interface*, *5*(27), 1137–1158. https://doi.org/10.1098/rsif.2008.0151
[30] Rezvani Sichani, H., Atapour, M., Ashrafizadeh, F., Galati, M., & Saboori, A. (2024). Mechanical, electrochemical and permeability behaviour of Ti6Al–4V scaffolds fabricated by electron beam powder bed fusion for orthopedic implant applications: The role of cell type and cell size. *Journal of Materials Research and Technology*, *28*, 3240–3257. https://doi.org/10.1016/j.jmrt.2023.12.260
[31] Yang, W., Yu, H., Liang, H., Li, D., & Zhang, Y. (2022). Properties of additive-manufactured open porous titanium structures for patient-specific load-bearing implants. *Frontiers in Mechanical Engineering*, *7*, Article 830126. https://doi.org/10.3389/fmech.2021.830126
[32] Liang, Y., Li, H., Xu, J., Li, X., Qi, M., & Hu, M. (2014). Biological properties of titanium cages modified with hydroxyapatite: A cellular and molecular analysis. *International Journal of Molecular Sciences*, *15*(6), 9952–9964. https://doi.org/10.3390/ijms15069952

[33] Krishna, B. V., Bose, S., & Bandyopadhyay, A. (2007). Fabrication of porous hydroxyapatite scaffolds by selective laser sintering and their interaction with osteoblast cells. *Acta Biomaterialia*, *3*(6), 997–1006. https://doi.org/10.1016/j.actbio.2007.04.007
[34] Alvarez, K., & Nakajima, H. (2009). Design of porous metallic materials for biomedical applications. *Materials*, *2*(2), 790–832. https://doi.org/10.3390/ma2020790
[35] Karageorgiou, V., & Kaplan, D. (2005). Porosity of 3D biomaterial scaffolds and osteogenesis. *Biomaterials*, *26*(27), 5474–5491. https://doi.org/10.1016/j.biomaterials.2005.02.002
[36] Matassi, F., Botti, A., Sirleo, L., Carulli, C., & Innocenti, M. (2013). Case series: Mineral bone metabolism in orthopedic care. *Clinical Cases in Mineral and Bone Metabolism*, *10*(2), 111–115.
[37] Bobyn, J. D., Pillar, R. M., Cameron, H. U., & Weatherly, G. C. (1980). The interface mechanics of porous-coated implants. *Clinical Orthopaedics and Related Research*, (*150*), 263–278.
[38] Zardiackas, L. D., Parsell, D. E., Dillon, L. D., Mitchell, D. W., Nunnery, L. A., & Poggie, R. (2001). Porous tantalum structures for orthopedic implants: Bone adaptation and mechanical properties. *Journal of Biomedical Materials Research*, *58*(2), 180–187. https://doi.org/10.1002/1097-4636(2001)58:2<180::AID-JBM1005>3.0.CO;2-5
[39] Levine, B. R., Sporer, S., Poggie, R. A., Della Valle, C. J., & Jacobs, J. J. (2006). Experimental and clinical performance of porous tantalum in orthopedic implants. *Biomaterials*, *27*(20), 4671–4678. https://doi.org/10.1016/j.biomaterials.2006.04.041
[40] Cohen, R. (2002). A porous tantalum trabecular metal: basic science. *American Journal of Orthopedics* (*Belle Mead, N.J.*), *31*(4), 216–217. PMID: 12008853
[41] Cohen, R. (2006). Experimental and clinical performance of porous tantalum in orthopedic surgery. *Biomaterials*, *27*(27), 4671–4678. https://doi.org/10.1016/j.biomaterials.2006.04.041
[42] Martin, P. M. (2010). Overview of film and coating deposition methods. In P. M. Martin (Ed.), *Handbook of deposition technologies for films and coatings* (3rd ed., pp. 1–18). William Andrew Publishing
[43] Hacking, S. A., Bobyn, J. D., Toh, K., Tanzer, M., & Krygier, J. J. (2000). The influence of porous tantalum structure on bone ingrowth and implant fixation. *Journal of Biomedical Materials Research*, *52*(4), 631–638.
[44] Lu, M., Xu, S., Lei, Z. X., Lu, D., Cao, W., Huttula, M., Hou, C. H., Du, S. H., Chen, W., Dai, S. W., Li, H. M., & Jin, D. D. (2019). Application of a novel porous tantalum implant in a rabbit anterior lumbar spine fusion model: in vitro and in vivo experiments. *Chinese Medical Journal* (*English*), *132*(1), 51–59. https://doi.org/10.1097/CM9.0000000000000030
[45] Tanzer, M., Kantor, S., & Bobyn, J. D. (2001). Enhancement of bone growth into porous-coated implants using non-invasive low intensity ultrasound. *Journal of Orthopaedic Research*, *19*(2), 195–199. https://doi.org/10.1016/S0736-0266(00)00034-6
[46] Bobyn, J. D., Toh, K. K., Hacking, S. A., Tanzer, M., & Krygier, J. J. (1999). Characterization of porous tantalum implants in animal models. *Journal of Biomedical Materials Research*, *4*, 347–354.
[47] Kim, D. G., Huja, S. S., Tee, B. C., Larsen, P. E., Kennedy, K. S., Chien, H. H., Lee, J. W., & Wen, H. B. (2013). Bone ingrowth and initial stability of titanium and porous tantalum dental implants: A pilot canine study. *Implant Dentistry, 22*(4), 399–405. https://doi.org/10.1097/ID.0b013e31829b17b5
[48] Battula, S., Lee, J. W., Wen, H. B., Papanicolaou, S., Collins, M., & Romanos, G. E. (2015). Evaluation of different implant designs in a ligature-induced peri-implantitis model: A canine study. *The International Journal of Oral & Maxillofacial Implants*, *30*(3), 534–545.doi:10.11607/jomi.3737.
[49] Lee, J. W., Wen, H. B., Gubbi, P., & Romanos, G. E. (2018). New bone formation and trabecular bone microarchitecture of highly porous tantalum compared to titanium implant threads: A pilot canine study. *Clinical Oral Implants Research, 29*(2), 164–174. doi:10.1111/clr.13074.
[50] Wang, Y., Xu, Y., Jiang, Y., Liu, L., & Yang, Y. (2022). Advances in surface modification of tantalum and porous tantalum for rapid osseointegration: A thematic review. *Frontiers in Bioengineering and Biotechnology*, *10*, 983695. https://doi.org/10.3389/fbioe.2022.983695
[51] Fu, W. M., Yang, L., Wang, B. J., Xu, J. K., Wang, J. L., Qin, L., & Zhao, D. W. (2016). Porous tantalum seeded with bone marrow mesenchymal stem cells attenuates steroid-associated osteonecrosis. *European review for medical and pharmacological sciences*, *20*(16), 3490–3499.
[52] Wu, L. C., Hsieh, Y. Y., Hsu, T. S., Liu, P. Y., Tsuang, F. Y., Kuo, Y. J., Chen, C. H., Van Huynh, T., & Chiang, C. J. (2024). 3D-printed porous titanium suture anchor: a rabbit lateral femoral condyle model. *BMC musculoskeletal disorders*, *25*(1), 559. https://doi.org/10.1186/s12891-024-07666-w
[53] Luo, C., Wang, C., Wu, X., Xie, X., Wang, C., Zhao, C., Zou, C., Lv, F., Huang, W., & Liao, J. (2021). Influence of porous tantalum scaffold pore size on osteogenesis and osteointegration: A comprehensive study based on 3D-printing technology. *Materials Science and Engineering: C*, 129, 112382. https://doi.org/10.1016/j.msec.2021.112382
[54] Wang, H., Su, K., Su, L., Liang, P., Ji, P., & Wang, C. (2019). Comparison of 3D-printed porous tantalum and titanium scaffolds on osteointegration and osteogenesis. *Materials Science and Engineering: C*, *104*, 109908. https://doi.org/10.1016/j.msec.2019.109908

[55] Bandyopadhyay, A., Mitra, I., Shivaram, A., Dasgupta, N., & Bose, S. (2019). Direct comparison of additively manufactured porous titanium and tantalum implants toward in vivo osseointegration. *Additive Manufacturing*, *28*, 259–266. https://doi.org/10.1016/j.addma.2019.04.025
[56] Zou, X., Xue, Q., Li, H., Bünger, M., Lind, M., & Bünger, C. (2003). Effect of alendronate on bone ingrowth into porous tantalum and carbon fiber interbody devices: An experimental study on spinal fusion in pigs. *Acta Orthopaedica*, *74*(5), 596–603. https://doi.org/10.1080/00016470310018027
[57] Zou, X., Li, H., Bünger, M., Egund, N., Lind, M., & Bünger, C. (2004). Bone ingrowth characteristics of porous tantalum and carbon fiber interbody devices: An experimental study in pigs. *The Spine Journal*, *4*(1), 99–106. https://doi.org/10.1016/S1529-9430(03)00407-8
[58] Fraser, D., Funkenbusch, P. D., Ercoli, C., & Meirelles, L. (2019). Bone response to porous tantalum implants in a gap-healing model. *Clinical Oral Implants Research*, *30*(2), 156–168. https://doi.org/10.1111/clr.13402
[59] Fraser, D., Funkenbusch, P., Ercoli, C., & Meirelles, L. (2019). Biomechanical analysis of the osseointegration of porous tantalum implants. *Journal of Prosthetic Dentistry, 123*(6), 811–820. https://doi.org/10.1016/j.prosdent.2019.09.014
[60] Mrosek, E. H., Chung, H. W., Fitzsimmons, J. S., O'Driscoll, S. W., Reinholz, G. G., & Schagemann, J. C. (2016). Porous tantalum biocomposites for osteochondral defect repair: A follow-up study in a sheep model. *Bone & Joint Research*, *5*(9), 403–411. https://doi.org/10.1302/2046-3758.59.BJR-2016-0070.R1
[61] Ren, B., Zhai, Z., Guo, K., Liu, Y., Hou, W., Zhu, Q., & Zhu, J. (2015). Porous tantalum-enhanced osteogenesis around implants. *International Journal of Clinical and Experimental Medicine*, *8*(3), 5055–5062. PMID: 26131078. Available at PubMed Central: https://www.ncbi.nlm.nih.gov/pmc/articles/PMC4483870/
[62] Albrektsson, T., & Johansson, C. (2001). Current interpretations of osseointegration. *European Spine Journal*, *10*(*Suppl 2*), S96–S101. https://doi.org/10.1007/s005860000292
[63] Koutsostathis, S. D., Tsakotos, G. A., Papakostas, I., & Macheras, G. A. (2009). Porous tantalum in orthopaedic surgery: Clinical perspectives. *Journal of Orthopaedics*, *6*, e3.
[64] Huang, B., Zou, X., Li, H., Xue, Q., & Bünger, C. (2013). Long-term performance of porous tantalum fusion cages in a goat cervical spine model. *European Spine Journal*, *22*(2), 287–297. https://doi.org/10.1007/s00586-012-2373-2
[65] Fan, H., Wang, G., Xiu, P., Wang, Y., & Yang, Y. (2021). Highly porous 3D-printed tantalum scaffolds have better biomechanical and microstructural properties than titanium scaffolds. *BioMed Research International*, *2021*, 2899043. https://doi.org/10.1155/2021/2899043
[66] Wei, et al. (2023). Fabrication of porous tantalum with low elastic modulus and tunable pore size for bone repair. *ACS Biomaterials Science & Engineering*, *9*, 23–34. https://doi.org/10.1021/acsbiomaterials.2c01239
[67] Bauer, T. W., & Schils, J. (1999). The pathology of total joint arthroplasty. *Skeletal Radiology*, *28*(8), 483–494. https://doi.org/10.1007/s002560050541
[68] Pokrass, C. (1990). *Tantalum in metals handbook*. In C. Pokrass (Ed.), Properties and Selection: Nonferrous Alloys and Special-Purpose Materials (Vol. 2, 10th ed., p. 571). ASM International.
[69] Black, J. (1994). Clinical applications of tantalum biomaterials. *Clinical Materials*, *16*(4), 167–173.
[70] Guo, Y., Xie, K., Jiang, W., Wang, L., Li, G., Zhao, S., Wu, W., & Hao, Y. (2019). In vitro and in vivo study of 3D-printed porous tantalum scaffolds for repairing bone defects. *ACS Biomaterials Science & Engineering*, *5*(2), 1123–1133. https://doi.org/10.1021/acsbiomaterials.8b01094
[71] Blanco, J. F., Sánchez-Guijo, F. M., Carrancio, S., Muntion, S., García-Briñon, J., & del Cañizo, M.-C. (2011). Titanium and tantalum as mesenchymal stem cell scaffolds for spinal fusion: An in vitro comparative study. *European Spine Journal*, *20*(*Suppl 3*), 353–360. https://doi.org/10.1007/s00586-011-1901-8
[72] Wang, H., Su, K., Su, L., Liang, P., Ji, P., & Wang, C. (2019). Comparison of 3D-printed porous tantalum and titanium scaffolds on osteointegration and osteogenesis. *Materials Science and Engineering: C*, *104*, 109908. https://doi.org/10.1016/j.msec.2019.109908
[73] Wei, X., Liu, B., Liu, G., Yang, F., Cao, F., Dou, X., Yu, W., Wang, B., Zheng, G., Cheng, L., Ma, Z., Zhang, Y., Yang, J., Wang, Z., Li, J., Cui, D., Wang, W., Xie, H., Li, L., Zhang, F., Lineaweaver, W. C., & Zhao, D. (2019). Mesenchymal stem cell–tantalum scaffold constructs accelerate bone regeneration. *Stem Cell Research & Therapy*, *10*, 72. https://doi.org/10.1186/s13287-019-1176-273
[74] Liu, A., Wang, C., Zhao, Z., Zhu, R., Deng, S., Zhang, S., ... Li, D. (2025). Progress of porous tantalum surface-modified biomaterial coatings in bone tissue engineering. *Journal of Materials Science: Materials in Medicine*, *36*(26). https://doi.org/10.1007/s10856-025-06871-w
[75] Liu, X., Xie, Y., Yang, F., Huang, Y., Wang, C., Dai, K., & Zhang, X. (2023). Preparation, modification, and clinical application of porous tantalum scaffolds. *Frontiers in Bioengineering and Biotechnology*, *11*, 112793. https://doi.org/10.3389/fbioe.2023.1127939
[76] Zhou, Z., & Liu, D. (2022). Mesenchymal stem cell-seeded porous tantalum-based biomaterial: A promising choice for promoting bone regeneration. *Colloids and Surfaces B: Biointerfaces*, *215*, 112491. https://doi.org/10.1016/j.colsurfb.2022.112491

[77] Sun, Y., Li, Z., Zhao, P., Huang, W., Liu, H., Li, Y., Zhou, J., Wang, K., & Zhang, C. (2022). Differential effects of tantalum nanoparticles versus tantalum microparticles on macrophage polarization in inflammatory microenvironments. *Biomaterials Advances*, *153*, 213345. https://doi.org/10.1016/j.mtbio.2022.100340

[78] Wang, Q., Zhang, H., Gan, H., Wang, H., Li, Q., & Wang, Z. (2018). Application of combined porous tantalum scaffolds loaded with bone morphogenetic protein 7 to repair of osteochondral defect in rabbits. *International Orthopaedics*, *42*(7), 1437–1448. https://doi.org/10.1007/s00264-018-3800-7

[79] Huang, B., Zou, X., Li, H., Xue, Q., & Bünger, C. (2013). Short-term alendronate treatment does not maintain a residual effect on spinal fusion with interbody devices and bone graft after treatment withdrawal: an experimental study on spinal fusion in pigs. *European spine journal : official publication of the European Spine Society, the European Spinal Deformity Society, and the European Section of the Cervical Spine Research Society*, *22*(2), 287–295. https://doi.org/10.1007/s00586-012-2513-7

[80] Dou, X., Wei, X., Liu, G., Wang, S., Lv, Y., Li, J., Ma, Z., Zheng, G., Wang, Y., Hu, M., Yu, W., & Zhao, D. (2019). Effect of porous tantalum on promoting the osteogenic differentiation of bone marrow mesenchymal stem cells in vitro through the MAPK/ERK signaling pathway. *Journal of Orthopaedic Translation*, *19*, 81–93. https://doi.org/10.1016/j.jot.2019.03.006

[81] Al Deeb, M., AlFarraj, A. A., & Anil, S. (2023). Osseointegration of Tantalum Trabecular Metal in Titanium Dental Implants: Histological and Micro-CT Study. *Journal of Functional Biomaterials*, *14*(7), 355. https://doi.org/10.3390/jfb14070355

[82] Cui, J., Zhang, S., Huang, M., Mu, X., Hei, J., Yau, V., & He, H. (2023). Micro-nano porous structured tantalum-coated dental implants promote osteogenic activity in vitro and enhance osseointegration in vivo. *Journal of biomedical materials research. Part A*, *111*(9), 1358–1371. https://doi.org/10.1002/jbm.a.37538

[83] Edelmann, A. R., Patel, D., Allen, R. K., Gibson, C. J., Best, A. M., & Bencharit, S. (2019). Immediate loading protocols using porous tantalum dental implants: A clinical evaluation. *Journal of Prosthetic Dentistry*, *121*(3), 404–412. https://doi.org/10.1016/j.prosdent.2018.04.022

[84] Bencharit, S., Morelli, T., Barros, S., Seagroves, J. T., Kim, S., Yu, N., Byrd, K., Brenes, C., & Offenbacher, S. (2019). Comparing Initial Wound Healing and Osteogenesis of Porous Tantalum Trabecular Metal and Titanium Alloy Materials. *The Journal of oral implantology*, *45*(3), 173–180. https://doi.org/10.1563/aaid-joi-D-17-00258

[85] Unger, A. S., Lewis, R. J., & Gruen, T. (2005). Evaluation of a porous tantalum uncemented acetabular cup in revision total hip arthroplasty—two- to four-year clinical and radiographic results. *Journal of Arthroplasty*, *20*(8), 1002–1010. https://doi.org/10.1016/j.arth.2005.01.023

[86] Haidemenopoulos, G. N., Malizos, K. N., Zervaki, A. D., & Bargiotas, K. (2017). Human bone ingrowth into a porous tantalum acetabular cup. AIMS Materials Science, 4(6), 1220–1230. https://doi.org/10.3934/matersci.2017.6.1220

[87] Moen, T. C., Ghate, R., Salaz, N., Ghodasra, J., & Stulberg, S. D. (2011). A monoblock porous tantalum acetabular cup has no osteolysis on CT at 10 years. Clinical orthopaedics and related research, 469(2), 382–386. https://doi.org/10.1007/s11999-010-1500-8

[88] Tsao, A. K., Roberson, J. R., Christie, M. J., Dore, D. D., Heck, D. A., Robertson, D. D., & Poggie, R. A. (2005). Cementless porous tantalum acetabular components in primary THA: 5-year follow-up. *Journal of Bone and Joint Surgery American*, *87*(1), 22–28.

[89] Huang, W., Gong, X., Sandiford, S., He, X., Li, F., Li, Y., Liu, Z., Qin, L., Yang, J., Zhu, S., Wang, J., Tu, X., Ye, L., & Hu, N. (2019). Outcome after a new porous tantalum rod implantation for treatment of early-stage femoral head osteonecrosis. *Annals of translational medicine*, *7*(18), 441. https://doi.org/10.21037/atm.2019.08.86

[90] Zhang, Y., Wang, Y., Wang, Z., Zhang, H., Liu, S., Lin, Y., Li, H., & Li, L. (2024). Biomechanical evaluation and surgical strategy analysis of a novel porous tantalum acetabular cup using finite element method. *Journal of Orthopaedic Surgery and Research*, *19*(1), 231. https://doi.org/10.1186/s13018-024-05416-1

[91] Zhao, D., Liu, B., Wang, B., Yang, L., Xie, H., Huang, S., Zhang, Y., & Wei, X. (2015). Autologous bone marrow mesenchymal stem cells associated with tantalum rod implantation and vascularized iliac grafting for the treatment of end-stage osteonecrosis of the femoral head. *BioMed Research International*, *2015*, 240506. https://doi.org/10.1155/2015/240506

[92] Kayani, B., Howard, L. C., Neufeld, M. E., Greidanus, N. V., Masri, B. A., & Garbuz, D. S. (2024). Porous tantalum metaphyseal cones for severe femoral and tibial bone defects in revision total knee arthroplasty are reliable for fixation at mean 5-year follow-up. *The Journal of Arthroplasty*, *39*(9), S374–S379. https://doi.org/10.1016/j.arth.2024.03.022

[93] Hadley, M. L., Harmer, J. R., Wright, B. H., Larson, D. R., Abdel, M. P., Berry, D. J., & Lewallen, D. G. (2024). Porous Tantalum Tibial Metaphyseal Cones in Revision Total Knee Arthroplasty: Excellent 10-Year Survivorship. *The Journal of arthroplasty*, *39*(8S1), S263–S269. https://doi.org/10.1016/j.arth.2024.04.059

[94] Piovan, G., Bori, E., Padalino, M., Pianigiani, S., & Innocenti, B. (2024). Biomechanical analysis of patient specific cone vs conventional stem in revision total knee arthroplasty. *Journal of orthopaedic surgery and research*, *19*(1), 439. https://doi.org/10.1186/s13018-024-04936-0

[95] Mao, S., Liu, Y., Wang, F., He, P., Wu, X., Ma, X., & Luo, Y. (2023). Design and biomechanical analysis of patient-specific porous tantalum prostheses for knee joint revision surgery. *International Journal of Bioprinting*, *9*(4), 735. https://doi.org/10.18063/ijb.73

[96] Zhang, C., Zhou, Z., Liu, N., Chen, J., Wu, J., Zhang, Y., Lin, K., & Zhang, S. (2023). Osteogenic differentiation of 3D-printed porous tantalum with nano-topographic modification for repairing craniofacial bone defects. *Frontiers in bioengineering and biotechnology*, *11*, 1258030. https://doi.org/10.3389/fbioe.2023.1258030

[97] Liu, A., Liao, H., Zhang, X., Deng, S., Wang, C., Zhao, Z., Jiang, G., Li, D., Hu, J., & Hu, Z. (2025). A novel tantalum scaffold promoting osteoporotic osseointegration by controlled immune regulation. *International Journal of Bioprinting*, *11*(2), 474–493. https://doi.org/10.36922/ijb.8595

[98] Jiao, J., Hong, Q., Zhang, D., Wang, M., Tang, H., Yang, J., Qu, X., & Yue, B. (2023). Influence of porosity on osteogenesis, bone growth and osteointegration in trabecular tantalum scaffolds fabricated by additive manufacturing. *Frontiers in Bioengineering and Biotechnology*, *11*, 1117954. https://doi.org/10.3389/fbioe.2023.1117954

[99] Yu, H., Xu, M., Duan, Q., Li, Y., Liu, Y., Song, L., Cheng, L., Ying, J., & Zhao, D. (2024). 3D-printed porous tantalum artificial bone scaffolds: fabrication, properties, and applications. *Biomedical materials (Bristol, England), 19*(4), 10.1088/1748-605X/ad46d2. https://doi.org/10.1088/1748-605X/ad46d2

[100] Zhao, Z., Wang, M., Shao, F., Liu, G., Li, J., Wei, X., Zhang, X., Yang, J., Cao, F., Wang, Q., Wang, H., & Zhao, D. (2021). Porous tantalum-composited gelatin nanoparticles hydrogel integrated with mesenchymal stem cell-derived endothelial cells to construct vascularized tissue in vivo. *Regenerative Biomaterials*, *8*(6), rbab051. https://doi.org/10.1093/rb/rbab051